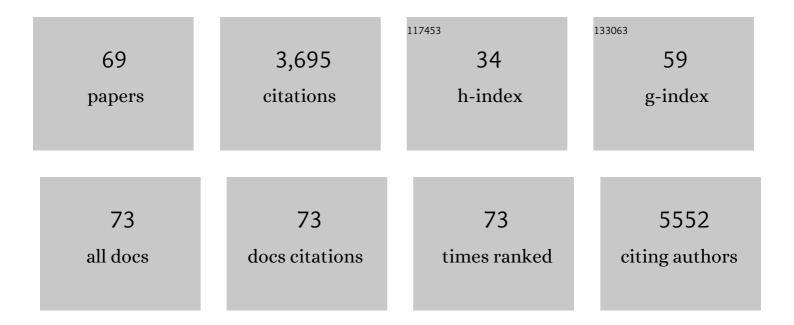
Samy Ould-Chikh

List of Publications by Year in descending order

Source: https://exaly.com/author-pdf/4064652/publications.pdf Version: 2024-02-01



SAMY OLILD-CHIKH

#	Article	IF	CITATIONS
1	Fe-MOF Materials as Precursors for the Catalytic Dehydrogenation of Isobutane. ACS Catalysis, 2022, 12, 3832-3844.	5.5	20
2	Unraveling the structure and role of Mn and Ce for NOx reduction in application-relevant catalysts. Nature Communications, 2022, 13, .	5.8	39
3	Active and stable Fe-based catalyst, mechanism, and key role of alkali promoters in ammonia synthesis. Journal of Catalysis, 2021, 394, 353-365.	3.1	16
4	Stable Cr-MFI Catalysts for the Nonoxidative Dehydrogenation of Ethane: Catalytic Performance and Nature of the Active Sites. ACS Catalysis, 2021, 11, 3988-3995.	5.5	34
5	Unlocking mixed oxides with unprecedented stoichiometries from heterometallic metal-organic frameworks for the catalytic hydrogenation of CO2. Chem Catalysis, 2021, 1, 364-382.	2.9	18
6	Multifunctional Catalyst Combination for the Direct Conversion of CO ₂ to Propane. Jacs Au, 2021, 1, 1719-1732.	3.6	25
7	Designing a Multifunctional Catalyst for the Direct Production of Gasoline-Range Isoparaffins from CO ₂ . Jacs Au, 2021, 1, 1961-1974.	3.6	22
8	The Comparison between Single Atom Catalysis and Surface Organometallic Catalysis. Chemical Reviews, 2020, 120, 734-813.	23.0	201
9	Development of catalysts for ammonia synthesis based on metal phthalocyanine materials. Catalysis Science and Technology, 2020, 10, 844-852.	2.1	22
10	Methane dry reforming on supported cobalt nanoparticles promoted by boron. Journal of Catalysis, 2020, 392, 126-134.	3.1	32
11	Role of Oxidized Mo Species on the Active Surface of Ni–Mo Electrocatalysts for Hydrogen Evolution under Alkaline Conditions. ACS Catalysis, 2020, 10, 12858-12866.	5.5	75
12	Metal–Organic Framework-Derived Synthesis of Cobalt Indium Catalysts for the Hydrogenation of CO ₂ to Methanol. ACS Catalysis, 2020, 10, 5064-5076.	5.5	88
13	Docking of tetra-methyl zirconium to the surface of silica: a well-defined pre-catalyst for conversion of CO ₂ to cyclic carbonates. Chemical Communications, 2020, 56, 3528-3531.	2.2	16
14	Coated sulfated zirconia/SAPO-34 for the direct conversion of CO ₂ to light olefins. Catalysis Science and Technology, 2020, 10, 1507-1517.	2.1	34
15	Mechanistic Study of Hydroamination of Alkyne through Tantalum-Based Silica-Supported Surface Species. ACS Catalysis, 2019, 9, 8719-8725.	5.5	15
16	Catalytic consequences of ultrafine Pt clusters supported on SrTiO3 for photocatalytic overall water splitting. Journal of Catalysis, 2019, 376, 180-190.	3.1	67
17	Maximizing Ag Utilization in High-Rate CO ₂ Electrochemical Reduction with a Coordination Polymer-Mediated Gas Diffusion Electrode. ACS Energy Letters, 2019, 4, 2024-2031.	8.8	85
18	Activity Descriptors Derived from Comparison of Mo and Fe as Active Metal for Methane Conversion to Aromatics. Journal of the American Chemical Society, 2019, 141, 18814-18824.	6.6	52

#	Article	IF	CITATIONS
19	Structure-activity relationships in metal organic framework derived mesoporous nitrogen-doped carbon containing atomically dispersed iron sites for CO2 electrochemical reduction. Journal of Catalysis, 2019, 378, 320-330.	3.1	36
20	A site-sensitive quasi-in situ strategy to characterize Mo/HZSM-5 during activation. Journal of Catalysis, 2019, 370, 321-331.	3.1	40
21	Turning a Methanation Co Catalyst into an In–Co Methanol Producer. ACS Catalysis, 2019, 9, 6910-6918.	5.5	88
22	On the reconstruction of NiMo electrocatalysts by <i>operando</i> spectroscopy. Journal of Materials Chemistry A, 2019, 7, 15031-15035.	5.2	24
23	Effect of Zeolite Topology and Reactor Configuration on the Direct Conversion of CO ₂ to Light Olefins and Aromatics. ACS Catalysis, 2019, 9, 6320-6334.	5.5	144
24	Tandem Conversion of CO ₂ to Valuable Hydrocarbons in Highly Concentrated Potassium Iron Catalysts. ChemCatChem, 2019, 11, 2879-2886.	1.8	57
25	A strategy to convert propane to aromatics (BTX) using TiNp ₄ grafted at the periphery of ZSM-5 by surface organometallic chemistry. Dalton Transactions, 2019, 48, 6611-6620.	1.6	6
26	TiO ₂ -supported Pt single atoms by surface organometallic chemistry for photocatalytic hydrogen evolution. Physical Chemistry Chemical Physics, 2019, 21, 24429-24440.	1.3	32
27	Synthesis of well-defined yttrium-based Lewis acids by capturing a reaction intermediate and catalytic application for cycloaddition of CO ₂ to epoxides under atmospheric pressure. Catalysis Science and Technology, 2019, 9, 6152-6165.	2.1	51
28	Tungsten Catalyst Incorporating a Wellâ€Defined Tetracoordinated Aluminum Surface Ligand for Selective Metathesis of Propane, [(≡Siâ^'Oâ''Si≡)(≡Siâ^'Oâ^') ₂ Alâ^'Oâ^'W(≡C <i>t</i> Bu) (H) ₂]. ChemCatChem, 2019, 11, 614-620.	1.8	2
29	Understanding of the structure activity relationship of PtPd bimetallic catalysts prepared by surface organometallic chemistry and ion exchange during the reaction of iso-butane with hydrogen. Journal of Catalysis, 2018, 363, 34-51.	3.1	9
30	A new high temperature reactor for operando XAS: Application for the dry reforming of methane over Ni/ZrO2 catalyst. Review of Scientific Instruments, 2018, 89, 035109.	0.6	13
31	Metal-Organic-Framework-Mediated Nitrogen-Doped Carbon for CO ₂ Electrochemical Reduction. ACS Applied Materials & amp; Interfaces, 2018, 10, 14751-14758.	4.0	105
32	A Silica-Supported Monoalkylated Tungsten Dioxo Complex Catalyst for Olefin Metathesis. ACS Catalysis, 2018, 8, 2715-2729.	5.5	38
33	On the dynamic nature of Mo sites for methane dehydroaromatization. Chemical Science, 2018, 9, 4801-4807.	3.7	65
34	Selective Production of Oxygenates from Carbon Dioxide Hydrogenation over a Mesoporousâ€5ilicaâ€5upported Copperâ€Gallium Nanocomposite Catalyst. ChemCatChem, 2018, 10, 1360-136	g.8	12
35	Precise Control of Pt Particle Size for Surface Structure–Reaction Activity Relationship. Journal of Physical Chemistry C, 2018, 122, 23451-23459.	1.5	8
36	Imine Metathesis Catalyzed by a Silica-Supported Hafnium Imido Complex. ACS Catalysis, 2018, 8, 9440-9446.	5.5	20

SAMY OULD-CHIKH

#	Article	IF	CITATIONS
37	Morphology control of anatase TiO2 for well-defined surface chemistry. Physical Chemistry Chemical Physics, 2018, 20, 14362-14373.	1.3	25
38	Physico-chemical investigation of ZnS thin-film deposited from ligand-free nanocrystals synthesized by non-hydrolytic thio-sol–gel. Nanotechnology, 2018, 29, 385603.	1.3	3
39	Metal Organic Framework-Derived Iron Catalysts for the Direct Hydrogenation of CO ₂ to Short Chain Olefins. ACS Catalysis, 2018, 8, 9174-9182.	5.5	155
40	Fe catalysts for methane decomposition to produce hydrogen and carbon nano materials. Applied Catalysis B: Environmental, 2017, 208, 44-59.	10.8	179
41	An Oxygenâ€Insensitive Hydrogen Evolution Catalyst Coated by a Molybdenumâ€Based Layer for Overall Water Splitting. Angewandte Chemie - International Edition, 2017, 56, 5780-5784.	7.2	106
42	An Oxygenâ€Insensitive Hydrogen Evolution Catalyst Coated by a Molybdenumâ€Based Layer for Overall Water Splitting. Angewandte Chemie, 2017, 129, 5874-5878.	1.6	13
43	In-operando elucidation of bimetallic CoNi nanoparticles during high-temperature CH4/CO2 reaction. Applied Catalysis B: Environmental, 2017, 213, 177-189.	10.8	88
44	On the "possible―synergism of the different phases of TiO2 in photo-catalysis for hydrogen production. Journal of Catalysis, 2017, 352, 657-671.	3.1	26
45	From single-site tantalum complexes to nanoparticles of Ta _x N _y and TaO _x N _y supported on silica: elucidation of synthesis chemistry by dynamic nuclear polarization surface enhanced NMR spectroscopy and X-ray absorption spectroscopy. Chemical Science, 2017, 8, 5650-5661.	3.7	14
46	The structure and binding mode of citrate in the stabilization of gold nanoparticles. Nature Chemistry, 2017, 9, 890-895.	6.6	222
47	SOMC-Designed Silica Supported Tungsten Oxo Imidazolin-2-iminato Methyl Precatalyst for Olefin Metathesis Reactions. Inorganic Chemistry, 2017, 56, 861-871.	1.9	23
48	Manufacture of highly loaded silica-supported cobalt Fischer–Tropsch catalysts from a metal organic framework. Nature Communications, 2017, 8, 1680.	5.8	128
49	Ni–M–O (M = Sn, Ti, W) Catalysts Prepared by a Dry Mixing Method for Oxidative Dehydrogenation of Ethane. ACS Catalysis, 2016, 6, 2852-2866.	5.5	120
50	Enhanced Kinetics of Hole Transfer and Electrocatalysis during Photocatalytic Oxygen Evolution by Cocatalyst Tuning. ACS Catalysis, 2016, 6, 4117-4126.	5.5	48
51	Single-Site VO _{<i>x</i>} Moieties Generated on Silica by Surface Organometallic Chemistry: A Way To Enhance the Catalytic Activity in the Oxidative Dehydrogenation of Propane. ACS Catalysis, 2016, 6, 5908-5921.	5.5	74
52	Optoelectronic and photovoltaic properties of the air-stable organohalide semiconductor (CH ₃ NH ₃) ₃ Bi ₂ I ₉ . Journal of Materials Chemistry A, 2016, 4, 12504-12515.	5.2	151
53	Transmission and fluorescence X-ray absorption spectroscopy cell/flow reactor for powder samples under vacuum or in reactive atmospheres. Review of Scientific Instruments, 2016, 87, 073108.	0.6	24
54	Methaneâ€induced Activation Mechanism of Fused Ferric Oxide–Alumina Catalysts during Methane Decomposition. ChemSusChem, 2016, 9, 1911-1915.	3.6	43

SAMY OULD-CHIKH

#	Article	IF	CITATIONS
55	VO _{<i>x</i>} /SiO ₂ Catalyst Prepared by Grafting VOCl ₃ on Silica for Oxidative Dehydrogenation of Propane. ChemCatChem, 2015, 7, 3332-3339.	1.8	30
56	Controlled Surface Segregation Leads to Efficient Cokeâ€Resistant Nickel/Platinum Bimetallic Catalysts for the Dry Reforming of Methane. ChemCatChem, 2015, 7, 819-829.	1.8	78
57	Ni–Ta–O mixed oxide catalysts for the low temperature oxidative dehydrogenation of ethane to ethylene. Journal of Catalysis, 2015, 329, 291-306.	3.1	57
58	Establishing Efficient Cobalt-Based Catalytic Sites for Oxygen Evolution on a Ta ₃ N ₅ Photocatalyst. Chemistry of Materials, 2015, 27, 5685-5694.	3.2	51
59	Photocatalysis with Chromiumâ€Doped TiO ₂ : Bulk and Surface Doping. ChemSusChem, 2014, 7, 1361-1371.	3.6	68
60	Facile and Efficient Synthesis of the Surface Tantalum Hydride (≡SiO) ₂ Ta ^{III} H and Tris-Siloxy Tantalum (≡SiO) ₃ Ta ^{III} Starting from Novel Tantalum Surface Species (≡SiO)TaMe ₄ and (≡SiO) ₂ TaMe ₃ . Organometallics, 2014, 3 1205-1211.	3 ^{1.1}	22
61	Critical Role of the Semiconductor–Electrolyte Interface in Photocatalytic Performance for Water-Splitting Reactions Using Ta ₃ N ₅ Particles. Chemistry of Materials, 2014, 26, 4812-4825.	3.2	98
62	Determination of the Electronic Structure and UV–Vis Absorption Properties of (Na2–xCux)Ta4O11 from First-Principle Calculations. Journal of Physical Chemistry C, 2013, 117, 17477-17484.	1.5	32
63	Understanding the key parameters for the rational design of layered oxide materials by composite sol–gel procedures. Powder Technology, 2013, 237, 255-265.	2.1	4
64	Synthesis of hierarchical anatase TiO2 nanostructures with tunable morphology and enhanced photocatalytic activity. RSC Advances, 2012, 2, 7048.	1.7	34
65	A New Approach to the Preparation of Nitrogen-Doped Titania Visible Light Photocatalyst. Chemistry of Materials, 2012, 24, 636-642.	3.2	70
66	Nb effect in the nickel oxide-catalyzed low-temperature oxidative dehydrogenation of ethane. Journal of Catalysis, 2012, 285, 292-303.	3.1	84
67	Hierarchical porous catalyst support: shaping, mechanical strength and catalytic performances. Studies in Surface Science and Catalysis, 2010, , 193-200.	1.5	6
68	Methodology of mechanical characterization of coated spherical materials. Powder Technology, 2009, 190, 19-24.	2.1	3
69	Pure silica-supported transition metal catalysts for the non-oxidative dehydrogenation of ethane: confinement effects on the stability. Journal of Materials Chemistry A, 0, , .	5.2	Ο